CONF-9305123--1

AN EMPIRICAL EQUATION FOR PENETRATION DEPTH OF OGIVE-NOSE PROJECTILES INTO CONCRETE TARGETS

M.J. Forrestal*, B.S. Altman*, J.D. Cargile†, S.J. Hanchak‡

*Sandia National Laboratories, Albuquerque, NM 87185-5800
†Waterways Experiment Station, Vicksburg, MS 39180-0631
‡University of Dayton Research Institute, Dayton, OH 45469-0182

RECEIVED
FEB 16 1993
OSTI
SAND--92-1948C
DE93 007604

ABSTRACT

We develop an empirical equation for penetration depth of ogive-nose projectiles penetrating concrete targets at normal impact. Our penetration equation contains a single, dimensionless empirical constant that depends only on the unconfined compressive strength of the target. We determine the empirical constant from penetration depth versus striking velocity data for targets with unconfined compressive strengths of nominally 14 MPa (2 ksi), 35 MPa (5 ksi), and 97 MPa (14 ksi). Predictions are in good agreement with six sets of penetration data for striking velocities between 250 and 800 m/s.

INTRODUCTION

Brown [1] presents an historical account of empirical equations for penetration and perforation of concrete targets. These empirical equations result from curve-fits with test data and do not provide physically based descriptions. In addition, the empirical equations in [1] are expressed in terms of specific units, so these equations are dimensionally dependent. In this paper, we develop a dimensionally consistent empirical equation for depth of penetration into concrete targets that contains the functional form of recently published, experimentally verified, analytical models [2,3,4].

MODEL FORMULATION

Forrestal and Luk [4] derive an analytical equation for penetration into soil targets that requires triaxial material data from samples cored from the target material. Unfortunately, most penetration studies lack the necessary triaxial test data required for input to analytical and computational models. Many experimental studies do, however, report the unconfined compressive strength f_c' for concrete targets. To use this data base, we develop an empirical penetration equation that describes the concrete targets in terms of unconfined compressive strength f_c', a dimensionless empirical constant S that multiplies f_c', and density ρ.

The development of the empirical equation starts with the equation for force on the projectile nose given in [4]. For the analytical model in [4] and this empirical equation, we assume normal impact and that the projectile is a rigid body (nondeforming nose). Axial force is given by

$$F = \pi a^2 \left(\tau_0 A + N B \rho V^2 \right) \tag{1a}$$

$$N = \frac{8\psi - 1}{24\psi^2} \tag{1b}$$

where the projectile has mass m, shank radius a, caliber-radius-head ψ, and rigid-body velocity V. The target is characterized by density ρ and the constants $(\tau_0 A)$ and B that involve only material parameters obtained from triaxial tests.

Previous studies [2,3,4] showed that B depends mostly on the compressibility of the target material and B has a narrow range; for example, $B = 1.1$ for aluminum targets [2,3], and $B = 1.2$ for soil targets [4]. By contrast, $(\tau_0 A)$ depends mostly on the shear strength of the target materials, and $(\tau_0 A)$ has a broad range. For this empirical equation, we take $B = 1$ and $(\tau_0 A) = Sf_c'$, where S is the dimensionless empirical constant that multiplies unconfined compressive strength. Thus, the empirical equation for axial force takes the form

$$F = \pi a^2\left(Sf_c' + N\rho V^2\right), \quad z > 4a \tag{2}$$

where N is given by equation (1b). Equation (2) is limited to penetration depths $z > 4a$. For $z < 4a$, the process is dominated by surface cratering.

Post-test observations of soil and concrete targets show that the cavity left after penetration has a conical region with length about two projectile shank diameters (4a) followed by a circular cylinder with diameter nearly equal to the projectile shank diameter (2a). Thus, the cavity length $0 < z < 4a$ is called the crater region, and the cavity length $4a < z < P$ is called the tunnel region, where z is measured from the target surface and P is final penetration depth. For the soil penetration tests analyzed in [4], $P \cong 100a$; so the crater region was ignored. However, both the crater and tunnel regions must be taken into account in the analysis of the more resistant concrete targets.

Deceleration data [4] show a rise time during the crater region, followed by a decaying pulse during the tunnel region. For this model, we take force on the projectile nose as

$$F = cz, \quad 0 < z < 4a \tag{3a}$$

$$F = \pi a^2\left(Sf_c' + N\rho V^2\right), \quad 4a < z < P \tag{3b}$$

where c is a constant. From Newton's second law

$$m\frac{d^2 z}{dt^2} = -cz, \quad 0 < z < 4a \tag{4}$$

With the initial conditions $z(t = 0) = 0$ and $V(t = 0) = V_s$, equation (4) has the following solutions for projectile displacement, velocity, and acceleration:

$$z = \left(\frac{V_s}{\omega}\right)\sin\omega t, \quad 0 < z < 4a \tag{5a}$$

$$V = \frac{dz}{dt} = V_s\cos\omega t, \quad 0 < z < 4a \tag{5b}$$

$$\frac{d^2 z}{dt^2} = -\omega V_s\sin\omega t, \quad 0 < z < 4a \tag{5c}$$

$$\omega^2 = \frac{c}{m} \tag{5d}$$

We now define t_1, and V_1 as the time and rigid-body projectile velocity at $z = 4a$. The unknowns t_1, V_1, and c are found from the conditions of continuity of force, velocity, and displacement at $z = 4a$ and $t = t_1$.

From equations (3 and 5)

$$m\omega V_s \sin \omega t_1 = \pi a^2\left(Sf_c' + N\rho V_1^2\right), \quad at\, z = 4a \tag{6a}$$

$$V_s \cos \omega t_1 = V_1, \quad at\, z = 4a \tag{6b}$$

$$\left(\frac{V_s}{\omega}\right)\sin \omega t_1 = 4a, \quad at\, z = 4a \tag{6c}$$

Substituting (6c) into (6a) gives

$$c = \frac{\pi a}{4}\left(Sf_c' + N\rho V_1^2\right) \tag{7a}$$

Squaring and then adding (6b) and (6c) give

$$c = \frac{m\left(V_s^2 - V_1^2\right)}{16a^2} \tag{7b}$$

Equating (7a) and (7b) gives the rigid-body velocity at $z = 4a$ as

$$V_1^2 = \frac{mV_s^2 - 4\pi a^3 Sf_c'}{m + 4\pi a^3 N\rho} \tag{7c}$$

From (6b),

$$t_1 = \frac{\cos^{-1}\left(\frac{V_1}{V_s}\right)}{\left(\frac{c}{m}\right)^{\frac{1}{2}}} \tag{7d}$$

Values of t_1, V_1, and c can be determined with equations (7b, c, and d).

Depth of penetration in the tunnel region is found from

$$m\frac{d^2 z}{dt^2} = mV\frac{dV}{dz} = -\pi a^2\left(Sf_c' + N\rho V^2\right), \quad 4a < z < P \tag{8}$$

Integrating (8) from V_1 to zero and $4a$ to P gives the final penetration depth

$$P = \frac{m}{2\pi a^2 \rho N} \ln\left(1 + \frac{N\rho V_1^2}{S f_c'}\right) + 4a, \quad P > 4a \tag{9}$$

where V_1 is related to the striking velocity V_s in equation (7c).

DETERMINATION OF EMPIRICAL CONSTANT FROM PENETRATION DATA

We solve for S and obtain

$$S = \frac{N\rho V_s^2}{f_c'} \bullet \frac{1}{\left(1 + \frac{4\pi a^3 N\rho}{m}\right) \exp\left[\frac{2\pi a^2 (P - 4a) N\rho}{m}\right] - 1} \tag{10}$$

For each experiment, all terms on the right side of equation (10) are known, so we can calculate S for each data point. We take the average value of S for the data points in each data set and compare results from equation (9) and penetration data. This procedure produced accurate data fits for six sets of penetration data.

14 MPa (2 ksi) Grout Targets.

Hanchak and Forrestal [5] conducted depth-of-penetration experiments with 0.064 kg, 12.7-mm-diameter projectiles with 3.0 and 4.25 caliber-radius-head nose shapes into grout targets. Table 1 lists the other parameters for these experiments. The value of S in Table 1 is the average of the values calculated from equation (10) for each data point. Figure 1 shows the results from equation (9) with $S = 21$ and the data sets with $\psi = 3.0$ and $\psi = 4.25$.

35 MPa (5 ksi) Concrete Targets.

Canfield and Clator [6] present depth-of-penetration data for full-scale (5.90 kg, 76.2-mm-diameter) and one-tenth scale (0.0059-kg, 7.62-mm-diameter) armor-piercing projectiles. Table 1 lists the other parameters for these experiments and the calculated value of S. Figures 2 and 3 show penetration data and results from equation (9) with $S = 13$ for the full-scale projectile and $S = 14$ for the one-tenth scale projectile.

Ehrgott and Cargile [7] conducted depth-of-penetration experiments with 0.90 kg, 26.9-mm-diameter projectiles. Table 1 lists the other parameters for these experiments and the calculated value of S. Figure 4 shows penetration data and results from equation (9) with $S = 12$.

97 MPa (14 ksi) Concrete Targets.

Ehrgott and Cargile [7] conducted depth-of-penetration experiments with 0.90 kg, 26.9-mm-diameter projectiles. Table 1 lists the other parameters for these experiments with the calculated value of S. Figure 4 shows penetration data and results from equation (9) with $S = 7$.

An Estimate for S versus f_c'

We obtained values of S for six data sets. For the two data sets with nominal 14 MPa (2 ksi) grout targets, $S = 21$; for the three data sets with nominal 35 MPa (5 ksi) concrete targets, S = 12, 13, and 14; and for the single data set with a nominal 97 MPa (14 ksi) concrete target, $S = 7$. The model prescribes that S depends only on f_c', and equation (10) shows that S is proportional to $1/f_c'$. Figure 5 shows the calculated values of S and a curve-fit where S is proportional to $1/f_c'$.

SUMMARY

We present a dimensionally consistent empirical equation for penetration depth of ogive-nose projectiles penetrating concrete targets. This equation has a single, dimensionless empirical constant S that multiplies unconfined compressive strength f_c'. The empirical constant S depends only on the unconfined compressive strength of the concrete target and is independent of the projectile parameters and striking velocity. We note that the penetration equation is limited to normal impact and rigid projectiles (nondeforming nose). Most of the penetration data base is limited to $V_s < 800$ m/s, and for $V_s < 800$ m/s, the nose remained undeformed.

ACKNOWLEDGEMENT

This work was supported by the Joint DoD/DOE Munitions Technology Development Program.

REFERENCES

1. S.J. Brown. Energy release protection for pressurized systems. Part II. Review of studies into impact/terminal ballistics. Applied Mechanics Reviews, Vol. 39, 1986.

2. M.J. Forrestal, N.S. Brar, and V.K. Luk. Penetration of strain-hardening targets with rigid spherical-nose rods. Journal of Applied Mechanics, Vol. 58, pp. 7-10, 1991.

3. M.J. Forrestal, V.K. Luk, Z. Rosenberg, and N.S. Brar. Penetration of 7075-T651 aluminum targets with ogival-nose rods. International Journal of Solids and Structures, Vol. 29, pp. 1729-1736, 1992.

4. M.J. Forrestal and V.K. Luk. Penetration into soil targets. International Journal of Impact Engineering, Vol. 12, pp. 427-444, 1992.

5. S.J. Hanchak and M.J. Forrestal. Penetration into grout targets with 0.064 kg, ogive-nose projectiles. Work in progress.

6. J.A. Canfield and I.G. Clator. Development of a scaling law and techniques to investigate penetration in concrete. NWL Report No. 2057, U.S. Naval Weapons Laboratory, Dahlgren, VA, 1966.

7. J.Q. Ehrgott and J.D. Cargile, Penetration into concrete targets. Work in progress.

Table 1. Penetration Parameters

Parameter	Ref. [5]	Ref. [5]	Ref. [6]	Ref. [6]	Ref. [7]	Ref. [7]
m (kg)	0.0642	0.0642	5.90	0.0059	0.906	0.904
2a (mm)	12.7	12.7	76.2	7.62	26.9	26.9
ψ	3	4.25	1.5	1.5	2.0	2.0
N	0.106	0.076	0.204	0.204	0.156	0.156
ρ (kg/m^3)	1960	1960	2310	2240	2370	2340
f'_c (MPa)	13.5	13.5	35.1	34.6	36.2	96.7
S	21	21	13	14	12	7

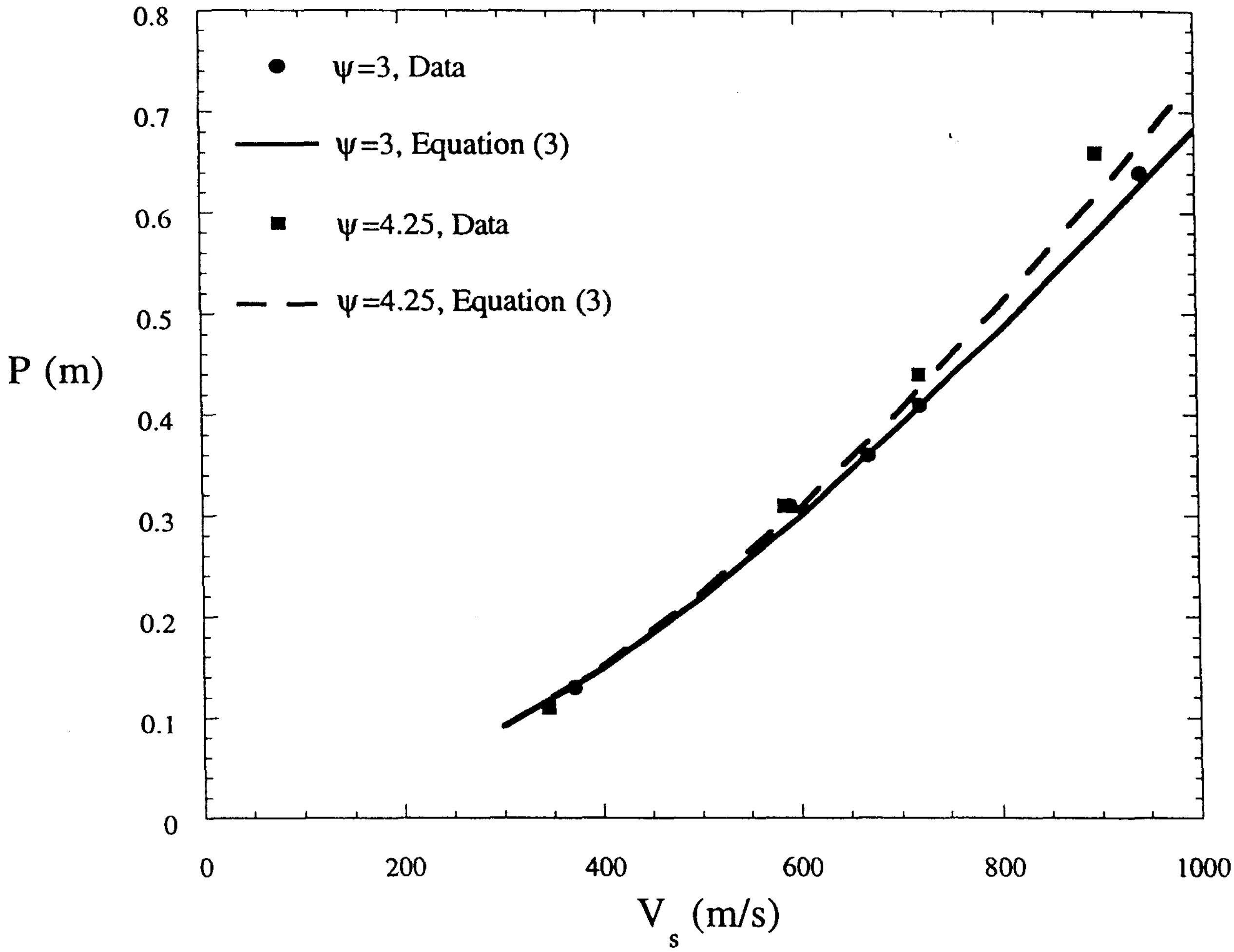

Figure 1. Penetration data [5] and model prediction for 0.064 kg, 12.7-mm-diameter projectile with f′c = 13.5 MPa, S=21.

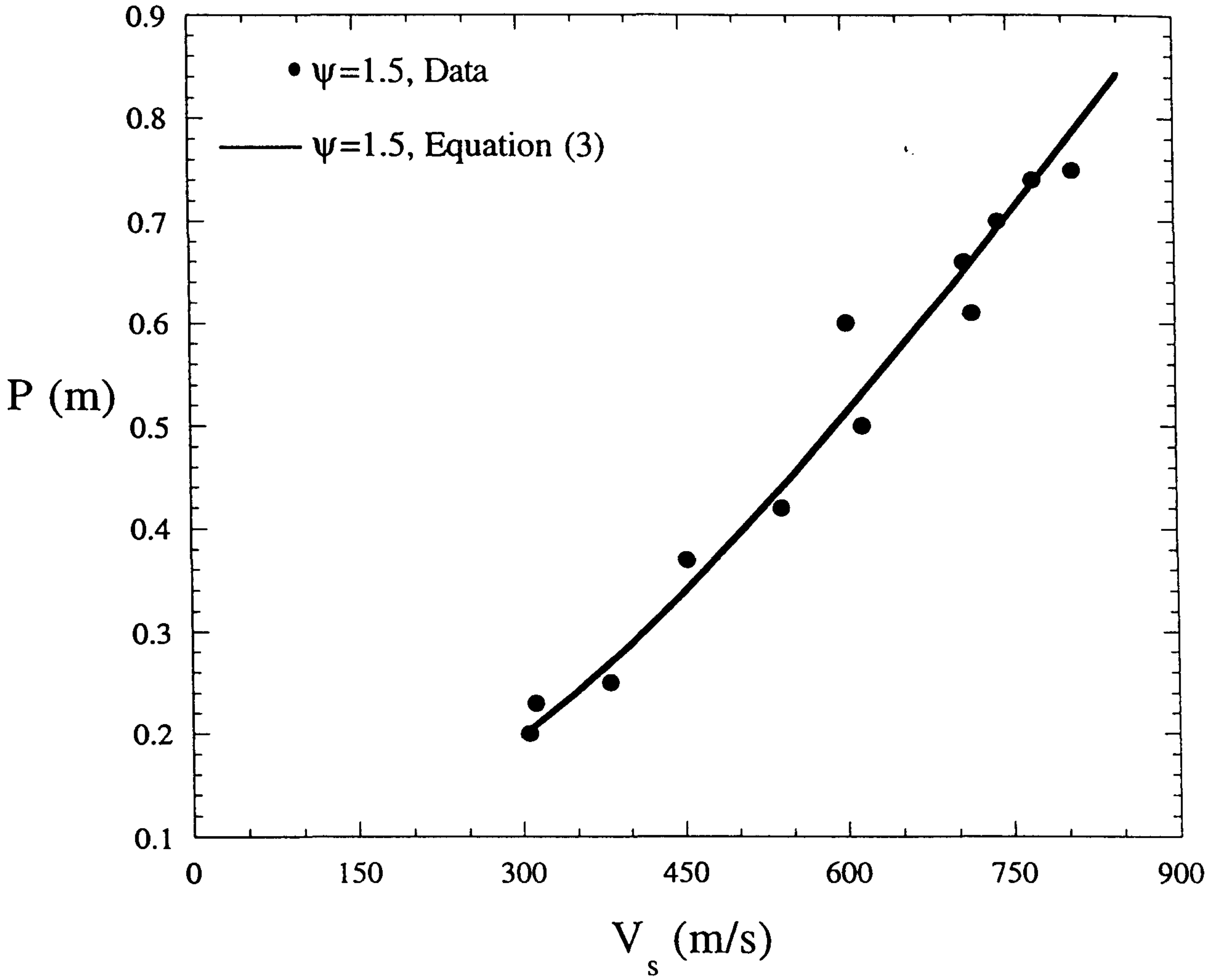

Figure 2. Penetration data [6] and model prediction for 5.9 kg, 76.2-mm-diameter projectile with f′c = 35.1 MPa, S=13.

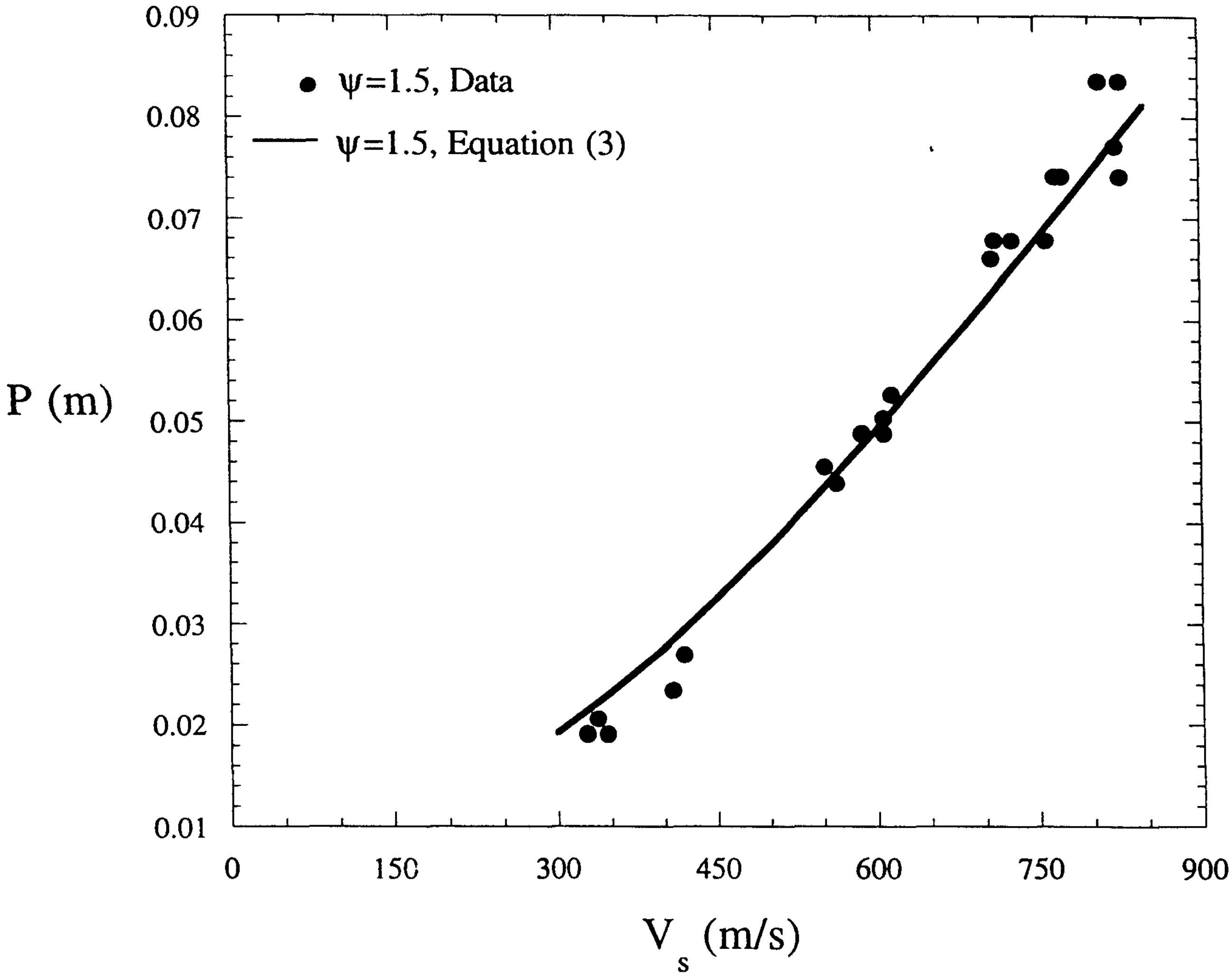

Figure 3. Penetration data [6] and model prediction for 0.0059 kg, 7.62-mm-diameter projectile with f′c = 34.6 MPa, S=14.

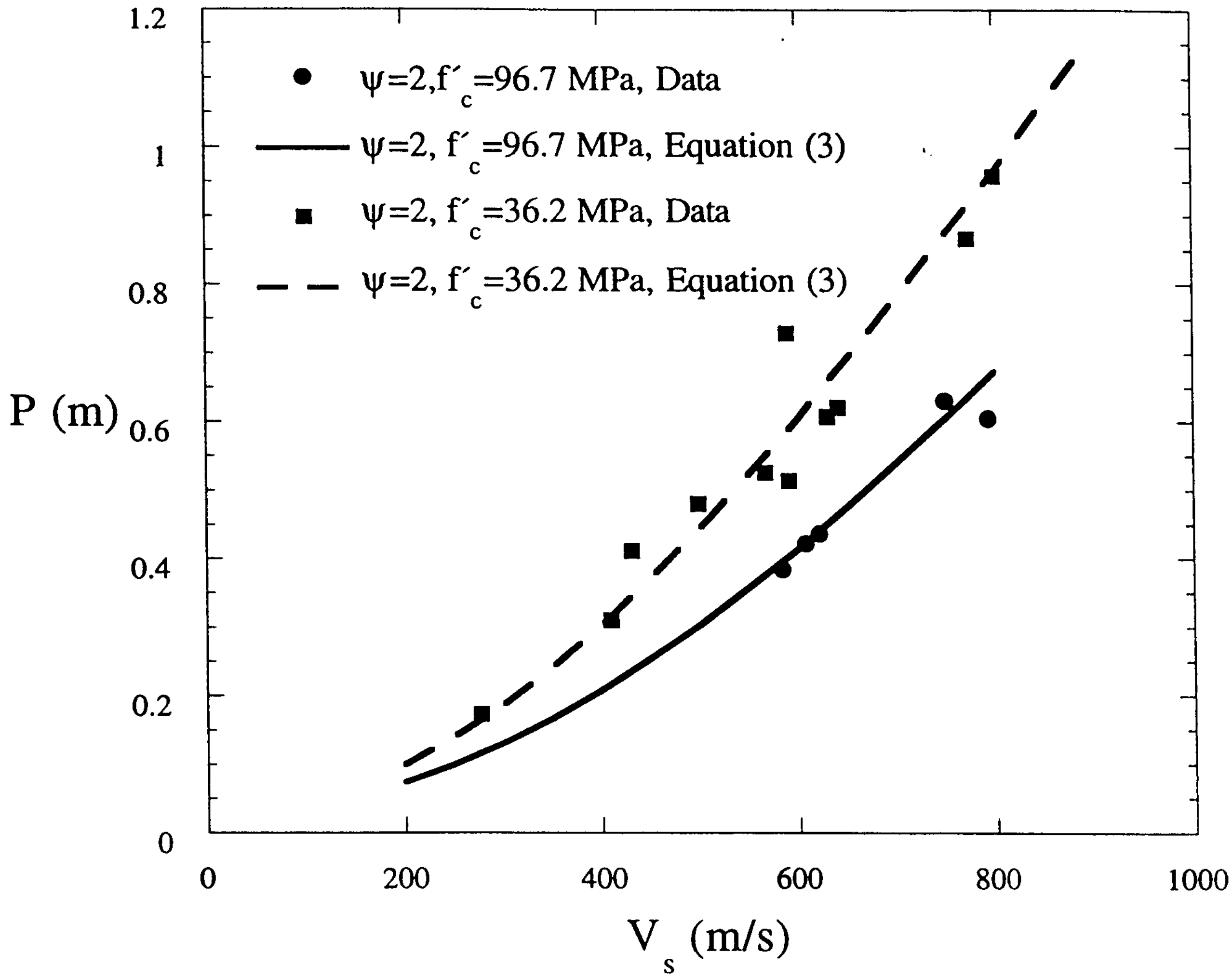

Figure 4. Penetration data [7] and model prediction for 0.904 kg, 26.9-mm-diameter projectile with f′c = 36.2 MPa, S=12 and f′c = 96.7 MPa, S=7.

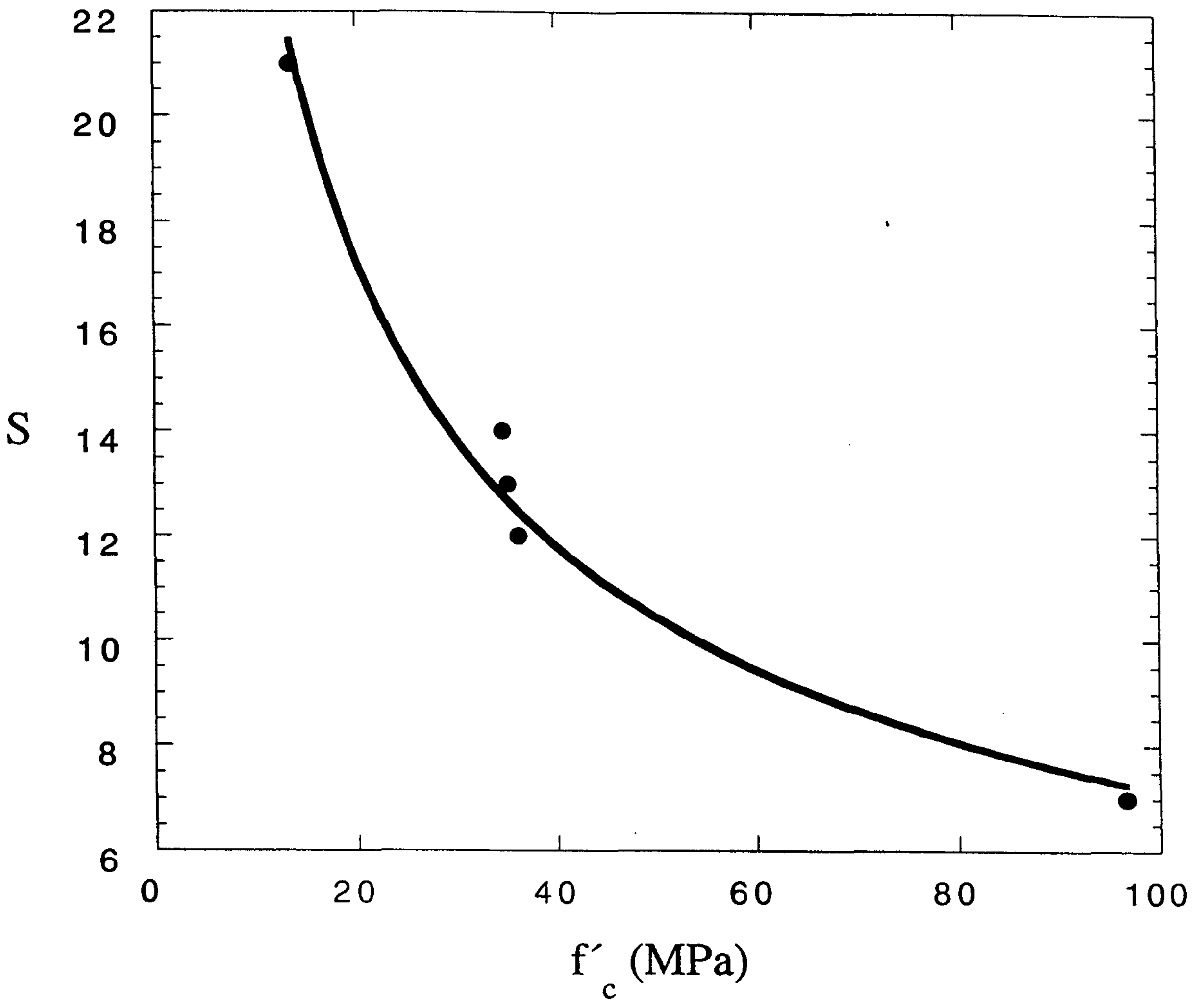

Figure 5. Dimensionless empirical constant versus unconfined compressive strength.